

Motional rotating wave approximation for harmonically trapped particles

Özgür E. Müstecaplıoğlu and L. You

School of Physics, Georgia Institute of Technology, Atlanta, GA 30332-0430, USA

(November 21, 2018)

We present a family of generalized unitary transformations that simplifies the Hamiltonian for a harmonically trapped two level atom (or ion) interacting with a plane wave laser field. Novel near resonant single as well as double vibrational phonon dynamical regimes are found. The validity condition of the often used motional rotating wave approximation (MRWA) is examined both numerically and analytically. Large errors are found within typical regimes of MRWA with respect to the motional degrees of freedom. The effects of MRWA in trapped ion systems are shown to be opposite to that of the rotating wave approximation (RWA) in the usual Jaynes-Cummings model. Our study points to a more restrictive condition on particle localization (Lamb-Dicke) parameter for the validity of MRWA in the single phonon dynamical regime. It also sheds new light on quantum information storage and processing with trapped atoms.

42.50.Ct, 42.50.Vk, 32.90.+a, 03.65.Ta

I. INTRODUCTION

In the last few years, much attention has been focused on quantum dynamics and coherence properties of trapped atoms or ions [1–5]. These studies led to many potentially attractive applications of harmonically trapped particles, e.g. in generating nonclassical vibrational phonons [6], implementing fast quantum gates [2], and in achieving phonon-ion entanglement [1]. In most of these studies, a coherent plane wave laser field near-resonantly couples two electronic states of an atom. The inclusion of motional degrees of freedom leads to tremendous complication. Several simplifications have been developed that reduce a trapped particle dynamics to the familiar Jaynes-Cummings Model (JCM) type form with the use of Lamb-Dicke limit (LDL), the strong confinement limit, or the motional rotating wave approximation (MRWA). In fact, the JCM description can be achieved regardless of laser field configuration, i.e. whether it is a travelling-wave [3] or a standing-wave [1,4]. LDL requires the particle localization size, given by the harmonic trap ground state width a , to be much less than the near resonant laser wavelength λ , i.e. $\eta = (2\pi)a/\lambda \ll 1$. It is often believed that MRWA for harmonically trapped particles works well within LDL as it demands a less restrictive condition $\eta \ll 2$ [3] or $\eta \ll 4$ [2].

In our ongoing effort to understand motional effects of trapped particles for quantum information processing [7], this issue of validity regimes for trapped particle MRWA again arises. We note some earlier investigations show that rotating wave approximation (RWA) does not work satisfactorily for Hamiltonians containing multiple transitions [8,9] or for systems initially prepared in a superposition of internal states [10]. Furthermore, multi-particle properties such as entanglement can have different sensitivity dependence on single particle MRWA [11]. With harmonically trapped particles, this issue becomes particularly acute as the equal distant motional states span an infinite dimensional Hilbert space. MRWA is typically made after a linearization by either taking LDL or by applying an exact simplifying unitary transformation. Within the latter approach, errors from MRWA can be further modified by the back transformation when dynamical observables are calculated in the original frame.

In this article we study quantum dynamics of a single trapped atom by employing a numerical diagonalization procedure without employing MRWA. We assess the validity regime for MRWA by comparing with results from analytical models obtained under MRWA. This paper is organized as follows. In Sec. II, our model system of a single trapped two level atom is described and a review of the unitary transformation method for linearizing the Hamiltonian is presented. The new result, the existence of a family of general unitary transformations for linearizing our model Hamiltonian, is then introduced. In Sec. III, we discuss two linearized models obtainable from our transformations. In Section IV, we outline several technical points about analytical solutions of the transformed model Hamiltonian under MRWA. We also discuss a numerical diagonalization procedure used for exact dynamic solutions. Selected results and comparisons are presented in Sec. V. Finally we conclude in Sec. VI.

II. THE MODEL SYSTEM AND A FAMILY OF GENERAL UNITARY TRANSFORMATIONS

To simplify our discussion, we consider a one-dimensional model of a harmonically trapped two level particle interacting with a near resonant laser field [3,12]. The system Hamiltonian is given by

$$\begin{aligned}
\mathcal{H} &= \mathcal{H}_0 + \mathcal{H}_1, \\
\mathcal{H}_0 &= \frac{P^2}{2M} + V_{tg}(x)\sigma_{gg} + [\hbar\omega_{eg} + V_{te}(x)]\sigma_{ee}, \\
\mathcal{H}_1 &= \frac{\Omega}{2}e^{i\hbar\omega_L t}e^{-ik_L x}\sigma_- + \text{H.c.}
\end{aligned} \tag{1}$$

where Ω , ω_L , and k_L denote respectively the Rabi frequency, carrier frequency, and wave number of a coherent driving laser. The electron transition frequency between excited ($|e\rangle$) and ground state ($|g\rangle$) is ω_{eg} . $\sigma_{ab} = |a\rangle\langle b|$ ($a/b = e, g$) are atomic projection operators. Consist with convention we denote $\sigma_- = |g\rangle\langle e|$ and $\sigma_z = \sigma_{ee} - \sigma_{gg}$. For a neutral particle, typically the approximate harmonic trap potential is internal state dependent, i.e. $V_{ta} = (1/2)M\nu_a^2 x^2$ with a corresponding trap frequency ν_a . P is the motional momenta and M is the mass of the particle.

We first simplify Eq. (1) by changing into the interaction picture (rotating frame) with the unitary transformation $\mathcal{H} \rightarrow e^{i\hbar\omega_L t\sigma_{ee}}\mathcal{H}e^{-i\hbar\omega_L t\sigma_{ee}} - \hbar\omega_L\sigma_{ee}$. This leads to

$$\begin{aligned}
\mathcal{H}_0 &= \frac{P^2}{2M} + V_{tg}(x) + \frac{\hbar\delta}{2}\sigma_z + [V_{te}(x) - V_{tg}(x)]\sigma_{ee} + \frac{\hbar\delta}{2}, \\
\mathcal{H}_1 &= \frac{\Omega}{2}e^{-ik_L x}\sigma_- + \text{H.c.},
\end{aligned} \tag{2}$$

where $\delta = \omega_{eg} - \omega_L$ is the laser field detuning. We now introduce motional phonon annihilation (creation) operator for the ground state a (a^\dagger) according to $P = \sqrt{\hbar M\nu_g/2}p$ and $x = \sqrt{\hbar/2M\nu_g}q$ with $p = i(a^\dagger - a)$ and $q = a^\dagger + a$. The displacement operator becomes $D(\beta) = e^{\beta a^\dagger - \beta^* a}$, and Eq. (2) simplifies to ($\hbar = 1$)

$$\begin{aligned}
\mathcal{H}_0 &= \nu_g n + \frac{\delta}{2}\sigma_z + \zeta q^2 \sigma_{ee} + \frac{\nu_g + \delta}{2}, \\
\mathcal{H}_1 &= \frac{\Omega}{2}D^\dagger(i\eta)\sigma_- + \text{H.c.},
\end{aligned} \tag{3}$$

where $n = a^\dagger a$ is the phonon number operator and $\zeta = (\nu_e^2 - \nu_g^2)/4\nu_g$. The Lamb-Dicke parameter is now $\eta = k_L\sqrt{1/2M\nu_g}$. For this particular form of the Hamiltonian, we note that its interaction part (\mathcal{H}_1) can be diagonalized by a general transformation matrix $\tilde{T} = E^\dagger T$, with

$$\begin{aligned}
E &= \frac{E_2 + E_1}{2}\hat{I} + \frac{E_2 - E_1}{2}\sigma_z, \\
T &= \frac{1}{\sqrt{2}}\left(\frac{D^\dagger(i\eta) + 1}{2}\hat{I} + \frac{D^\dagger(i\eta) - 1}{2}\sigma_z + \sigma_+ - D^\dagger(i\eta)\sigma_-\right).
\end{aligned} \tag{4}$$

We choose $\Omega \in \Re$ without loss of generality. It is easy to check that $\tilde{T}\mathcal{H}_1\tilde{T}^\dagger = (\Omega/2)\sigma_z$, is independent of the arbitrary unitary functional operators $E_{1,2}$ of a and a^\dagger . For any operator Θ , the transformed operator will be denoted to be $\tilde{\Theta} = \tilde{T}\Theta\tilde{T}^\dagger$. $\hat{I} = \sigma_{ee} + \sigma_{gg}$ is the identity operator. This transformation can be compared to the generalized Power-Zienau transformation discussed earlier [13]. In the phonon Fock state basis, it generates coherent superpositions of motional wave-packet states which was previously used in studying motional decoherence of atomic qubit operations [7]. It reduces to a simplifying transformation used by Moya-Cessa *et al.* [3] when we take $E_1 = E_2 = D(-i\eta/2)$. The \tilde{T} transformation on the \mathcal{H}_0 term can be conveniently calculated using the following properties

$$\begin{aligned}
D(\alpha)D(\beta) &= e^{(\alpha\beta^* - \alpha^*\beta)/2}D(\alpha + \beta), \\
D(\mp i\eta)a^\dagger a D(\pm i\eta) &= a^\dagger a \pm i\eta(a^\dagger - a) + \eta^2,
\end{aligned} \tag{5}$$

for arbitrary complex numbers α and β . We note that Eq. (5) simplifies to $D(\alpha)D(\beta) = D(\alpha + \beta)$ when α and β are purely imaginary. The second and the last term in the rhs of Eq. (6) correspond to the Doppler and recoil shifts. After this general transformation, we obtain

$$\tilde{\mathcal{H}}_0 = E^\dagger \left[(\nu_g n + gp + \eta g + \frac{\delta + \nu_g}{2} + \frac{\zeta}{2}q^2)\hat{I} - (gp + \frac{\zeta}{2}q^2 + \eta g + \frac{\delta}{2})\sigma_x \right] E, \tag{7}$$

with $g = \eta\nu_g/2$ and $\sigma_x = \sigma_+ + \sigma_-$. Different simplifications can be pursued by exploiting other forms of $E_{1,2}$. We note that the first term in Eq. (7) is in the form of a squeezed displaced harmonic oscillator. Therefore it can be diagonalized in the Fock state basis by the squeezed coherent state transformation $E_2 = E_1 = D(\beta)S(\xi)$. To eliminate

the p dependence in the coefficient of \hat{I} we choose $\beta = -i\eta/2$, which transforms according to $n \rightarrow n - (\eta/2)p + \eta^2/4$, $p \rightarrow p - \eta$, and $q \rightarrow q$. We then obtain

$$\tilde{\mathcal{H}}_0 = S^\dagger(\xi) \left[\left(\nu_g n + \frac{\zeta}{2} q^2 + \frac{\delta + \nu_g + \eta g}{2} \right) \hat{I} - \left(gp + \frac{\zeta}{2} q^2 + \frac{\delta}{2} \right) \sigma_x \right] S(\xi). \quad (8)$$

The squeezing transformation $S(\xi = re^{i\theta})$ causes $a \rightarrow ua^\dagger - v^*a$ with $u = \cosh r$ and $v = e^{i\theta} \sinh r$. For our model, ζ is required to be real, i.e. $\theta = 0$. The action of S results in

$$\begin{aligned} p &\rightarrow e^r p, \\ q &\rightarrow e^{-r} q, \\ n &\rightarrow e^{2r} n - \frac{1}{2} \sinh 2r q^2 + e^r \sinh r. \end{aligned} \quad (9)$$

Substitution these results into Eq. (8) leads to the elimination of the q^2 term in the coefficient of \hat{I} term provided we choose $r = (\ln \epsilon)/4$ with $\epsilon = 1 + 2\zeta/\nu_g$. This yields

$$\tilde{\mathcal{H}}_0 = \left[\nu_g \sqrt{\epsilon} n + \frac{\nu_g \sqrt{\epsilon} + g\eta + \delta}{2} \right] \hat{I} - \left(g\epsilon^{1/4} p + \frac{\zeta}{2\sqrt{\epsilon}} q^2 + \frac{\delta}{2} \right) \sigma_x. \quad (10)$$

We can now redefine parameters according to $\nu = \nu_g \sqrt{\epsilon}$, $g \rightarrow g\epsilon^{1/4}$, and $\zeta \rightarrow \zeta/\sqrt{\epsilon}$. Finally we arrive at the transformed Hamiltonian

$$\tilde{\mathcal{H}} = \nu n + \frac{\Omega}{2} \sigma_z - \left(gp + \frac{\zeta}{2} q^2 + \frac{\delta}{2} \right) \sigma_x, \quad (11)$$

where the constant term in the coefficient of \hat{I} has been dropped. We note that for ions with internal state independent trap frequencies $\zeta = r = \xi = 0$. We recover the same result as in Ref. [3] by choosing $\beta = -i\eta/2$. The effects of different trap frequencies for different internal levels are a renormalization of energy parameters in the single vibrational phonon Hamiltonian and a double vibrational phonon interaction through a term quadratic in the position operator. Double phonon transitions are the typical interactions that can lead to squeezed and entangled states for the vibrational phonons. In the next section, we will see that such two-phonon transitions can be dominated the single-phonon transitions in the system, independent of the Lamb-Dicke parameter η .

III. MOTIONAL ROTATING WAVE APPROXIMATION

The simplified model Hamiltonian Eq. (11) is of the form of a generalized JCM involving quadratic two-phonon transitions. It can be analytically solved for small squeezing parameters without external drive ($\Omega = 0$) [14]. Alternatively, when $|\nu - \Omega| \ll \Omega$ or $|2\nu - \Omega| \ll \Omega$, and g and $\zeta \ll \Omega$, an approximate analytic solution can be obtained by an explicit diagonalization upon the elimination of the rapidly oscillating terms, i.e. the application of MRWA. In the interaction picture, Eq. (11) becomes

$$\tilde{\mathcal{H}}_I = \left[-ig(a^\dagger e^{i\nu t} - a e^{-i\nu t}) + \frac{\zeta}{2}(a^{\dagger 2} e^{i2\nu t} + a^\dagger a + h.c.) + \frac{\delta}{2} \right] (\sigma_+ e^{i\Omega t} + \sigma_- e^{-i\Omega t}). \quad (12)$$

There exist two resonance conditions, one at $\Omega = \nu$ where the validity condition for MRWA becomes $(\eta\nu_g/2)\epsilon^{1/4} \ll \nu_g\epsilon^{1/2}$ [14], i.e. $\eta \ll 2\epsilon^{1/4}$. When the difference in trap frequencies is small we get $\eta \ll 7/4 + (\nu_e/2\nu_g)^2$. We see the validity regime of MRWA depends on η for this case of single phonon JCM. Physically the trap frequency difference can be controlled experimentally [15]. When $\nu_e = \nu_g$ as for an ion, we recover the condition $\eta \ll 2$ as discussed by Moya-Cessa *et al.* [3]. Under this condition, we arrive at the single phonon model

$$\begin{aligned} \tilde{\mathcal{H}}_{MRWA}^{(1p)} &= \mathcal{H}_{\text{free}}^{(1p)} + V^{(1p)}, \\ \mathcal{H}_{\text{free}}^{(1p)} &= \nu a^\dagger a + \frac{\nu}{2} \sigma_z, \\ V^{(1p)} &= -ig(a^\dagger \sigma_- - a \sigma_+). \end{aligned} \quad (13)$$

This Hamiltonian is the same with the Jaynes-Cummings model $H_{\text{JCM}} = \nu a^\dagger a + (\nu/2)\sigma_z - gp\sigma_x$ with the counter-rotating terms $a^\dagger \sigma_+, a \sigma_-$ are dropped under RWA.

Alternatively, there is a second resonance at $\Omega = 2\nu$. The condition for MRWA in this case is $\zeta/2 \ll \Omega$ [16], which becomes $7\nu_e^2 + 9\nu_g^2 \gg 0$. Hence, the validity regime of MRWA becomes independent of η in this case and can be realized simply by choosing larger trap frequencies. In contrast to the single phonon JCM in Eq. (13), the two phonon squeezing model can be achieved beyond LDL and is described by

$$\begin{aligned}\tilde{\mathcal{H}}_{MRWA}^{(2p)} &= \mathcal{H}_{\text{free}}^{(2p)} + V^{(2p)}, \\ \mathcal{H}_{\text{free}}^{(2p)} &= \nu a^\dagger a + \nu \sigma_z, \\ V^{(2p)} &= \frac{\zeta}{2}(a^{\dagger 2} \sigma_- + a^2 \sigma_+).\end{aligned}\tag{14}$$

Equations Eq. (13) and Eq. (14) consist the major results of the general unitary transform introduced earlier. Their complete dynamics, however, can be complicated as transformation back into the original Schrodinger picture induces coherent mixing of different states. In particular, if the system is initially prepared in a state $\psi(0)$, the linearized model Hamiltonian Eq. (13) has an initial state $\tilde{\psi}(0) = T\psi(0)$, which is always a superposition of both internal states. In other words, even for systems initially in only one internal state such that it has a vanishing dipole moment, the transformed system will always have a non-vanishing dipole-moment. It is known in this case that counter rotating terms (CRT) neglected in making MRWA become more significant and validity regimes for MRWA more restricted [10].

We are now in a position to discuss validity regimes of the commonly used MRWA for the simplified model Hamiltonians Eqs. (13) and (14). We will focus on the single-phonon model in Eq. (13) as it can be compared directly to existing results (under MRWA) in literature [3]. Furthermore, while the single phonon JCM can be obtained for small restricted values of the Lamb-Dicke parameter, two-phonon model is obtained without any restriction on the Lamb-Dicke parameter. Thus, determining the validity regime of MRWA is more essential for the single-phonon JCM.

IV. NUMERICAL METHOD

In the following discussion we focus on the single-phonon model and thus ignore the unnecessary superscript (1p) for notational simplicity. In the numerical studies, for the approximate JCM Eq. (13) we propagate any given initial states according to $\tilde{\psi}(t) = e^{-i\mathcal{H}_{\text{free}}t}U_I(t)\tilde{\psi}(0)$ with the known propagator $U_I(t) = e^{-itV}$ in the interaction picture [17],

$$U_I(t) = \frac{1}{\sqrt{2}} \begin{pmatrix} \cos[gt\sqrt{aa^\dagger}] & \sin[gt\sqrt{aa^\dagger}] \frac{a}{\sqrt{aa^\dagger}} \\ -\frac{a^\dagger}{\sqrt{aa^\dagger}} \sin[gt\sqrt{aa^\dagger}] & \cos[gt\sqrt{aa^\dagger}] \end{pmatrix}.\tag{15}$$

Transformed states are denoted by $\tilde{\psi} = \tilde{T}\psi$. In the Schrodinger picture, where observables are computed, the wave function becomes $\psi(t) = \tilde{T}^\dagger e^{-i\mathcal{H}_{\text{free}}t}U_I(t)\tilde{T}\psi(0)$. For example, the mean phonon number $\langle a^\dagger a \rangle$ is found to be

$$\langle n \rangle = \psi(0)^\dagger \tilde{T}^\dagger U_I^\dagger e^{i\mathcal{H}_{\text{free}}t} \tilde{T} a^\dagger a \tilde{T}^\dagger e^{-i\mathcal{H}_{\text{free}}t} U_I(t) \tilde{T} \psi(0),\tag{16}$$

which can be further simplified with the use of displacement operator property

$$\tilde{T} a^\dagger a \tilde{T}^\dagger = (a^\dagger a + \frac{\eta^2}{2}) \hat{I} - i \frac{\eta}{2} (a^\dagger - a) \sigma_x.\tag{17}$$

We note that the last term in the above Eq. involves momentum operator. Therefore, it does not commute with \mathcal{H}_0 and introduces fast oscillations due to the $e^{-i2\nu t}$ factor. We finally get,

$$\langle n \rangle = \tilde{\psi}(0)^\dagger U_I^\dagger \left[(a^\dagger a + \frac{\eta^2}{2}) \hat{I} - i \frac{\eta}{2} (a^\dagger e^{i\nu t} - a e^{-i\nu t}) (\sigma_+ e^{i\Omega t} + \sigma_- e^{-i\Omega t}) \right] U_I \tilde{\psi}(0).\tag{18}$$

We immediately see that CRT contribute to the dynamics of $\langle n \rangle$ because of multiple transitions in the original Hamiltonian. In addition to $\langle n \rangle$, CRT also affect other dynamical variables of interest, e.g. the Mandel-Q factor $(\langle (a^\dagger a)^2 \rangle - \langle a^\dagger a \rangle^2)/2$, which characterizes phonon statistics and the impurity factor $\mathcal{I} = 1 - \text{tr}(\rho_p^2)$ [18]. ρ_p is the reduced density operator in the phonon subsystem.

When all CRT are included, i.e. no MRWA is made, it is no longer possible to solve dynamic propagation analytically. However, the transformed Hamiltonian can be diagonalized numerically in a truncated phonon Fock state basis. It is easy to check the accuracy of such a truncation by testing for convergence with successively larger basis states. For an

initial Poisson distribution of vibrational phonons, the dimension of the truncated space becomes small enough that efficient algorithms are readily available. To illustrate this, let us consider an initial state where the particle is in the internal state $|e\rangle$ with a motional coherent state $|\alpha\rangle$, i.e. $\psi(0) = |e\rangle|\alpha\rangle$. The transformed initial condition becomes

$$\tilde{\psi}(0) = e^{-i\eta\Re(\alpha)} \frac{|e\rangle - |g\rangle}{\sqrt{2}} |\alpha - i\frac{\eta}{2}\rangle. \quad (19)$$

In a truncated Fock space of dimension N ($\gg |\alpha - i\eta/2|^2$), the state vector is expanded as

$$\tilde{\psi}(t) = \sum_{n=1, \Lambda=e, g}^N X_{n+n_\Lambda}(t) |\Lambda n\rangle, \quad (20)$$

with $n_\Lambda = 0, N$ and $\Lambda = e, g$ respectively. The initial condition (19) then becomes

$$X_{n+n_\Lambda}(0) = s_\Lambda \frac{1}{\sqrt{2}} e^{-i\eta\Re(\alpha)} F_{n-1}(\alpha - i\frac{\eta}{2}), \quad (21)$$

with $s_\Lambda = +1, -1$. The coherent state probability amplitudes in Fock space are $F_n(\alpha) = \exp(-|\alpha|^2/2) \alpha^n / \sqrt{n!}$. After back transformation, the original state vector evolution is then determined by

$$\psi(t) = \sum_{n=1, \Lambda=e, g} A_{n+n_\Lambda}(t) |\Lambda n\rangle, \quad (22)$$

with coefficients A_j for ($j = 1, 2, \dots, 2N$) given by

$$A_{n+n_\Lambda}(t) = \frac{1}{\sqrt{2}} \sum_{m=1}^N D_{n-1, m-1}(s_\Lambda \frac{\eta}{2}) [X_m(t) + s_\Lambda X_{m+N}(t)]. \quad (23)$$

The displacement operator matrix elements in Fock basis are known analytically in terms of Laguerre polynomials [19]. Therefore, the complete time evolution is obtained provided the transformed Hamiltonian is diagonalized. This is achieved through the standard expression

$$X_{i=1, \dots, N}(t) = \sum_{j, k=1}^{2N} V_{ij} V_{jk}^{-1} e^{-iW_j t} X_k(0), \quad (24)$$

where W_j are the eigenvalues of the transformed Hamiltonian and V is the diagonalizing matrix whose columns are the corresponding eigenvectors. In the following section we will compare MRWA results with the numerical diagonalization method (NDM).

V. RESULTS AND DISCUSSIONS

We focus in this section on the comparison of exact numerical results with results from MRWA for an initial motional coherent state $|\alpha\rangle$ with $\alpha = |\alpha| \exp(i\beta)$. Moya-Cessa *et al.* [3] have discussed a restricted form of the unitary transformation that led to a similar linearized model Hamiltonian earlier. Although formally independent of the Lamb Dicke parameter, their results were obtained under MRWA. In this first example, we demonstrate that their illustrative figure as presented in Ref. [3] is in fact invalid at the presumed marginal LDL $\eta = 0.5$. In Fig. 1, we see that MRWA result predicts regular behaviors for several dynamical variables, while the exact result from the NDM at $\eta = 0.5$ and $\alpha = (0.5, 5)$ display significant differences. In general we find that with NDM, the initial state losses its purity faster and ends up with a larger value for the time averaged mean phonon number. On the other hand, MRWA results typically give larger widths of temporal fluctuations for the Mandel-Q factor, especially at earlier times. Perhaps most importantly, MRWA results predict super-revivals [3] in Q and $\langle n \rangle$ that were never observed with NDM.

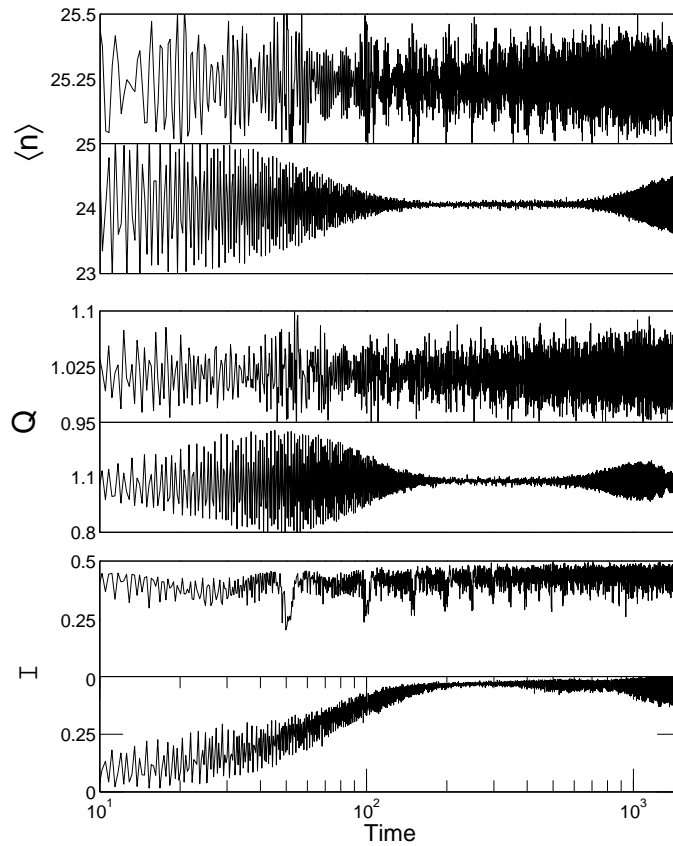


FIG. 1. Comparison of the mean phonon number $\langle n \rangle$, the Mandel-Q factor, and the impurity parameter \mathcal{I} for $\eta = 0.5$ and $\alpha = (0.5, 5)$. Always, the upper sub-figures are from the exact numerical diagonalization, while the lower ones are from MRWA. Time axis is in dimensionless from (scaled by $g = \eta\nu/2$). Note the differences as compared with Ref. [3].

Differences of similar orders of magnitude are also found for $\alpha = (5, 0.5)$ as detailed in Fig. 2. We also note the significantly improved quantitative agreement for $\langle n \rangle$ in this case. In fact, such improved agreement with MRWA results always seem to occur when $\beta \approx 0$.

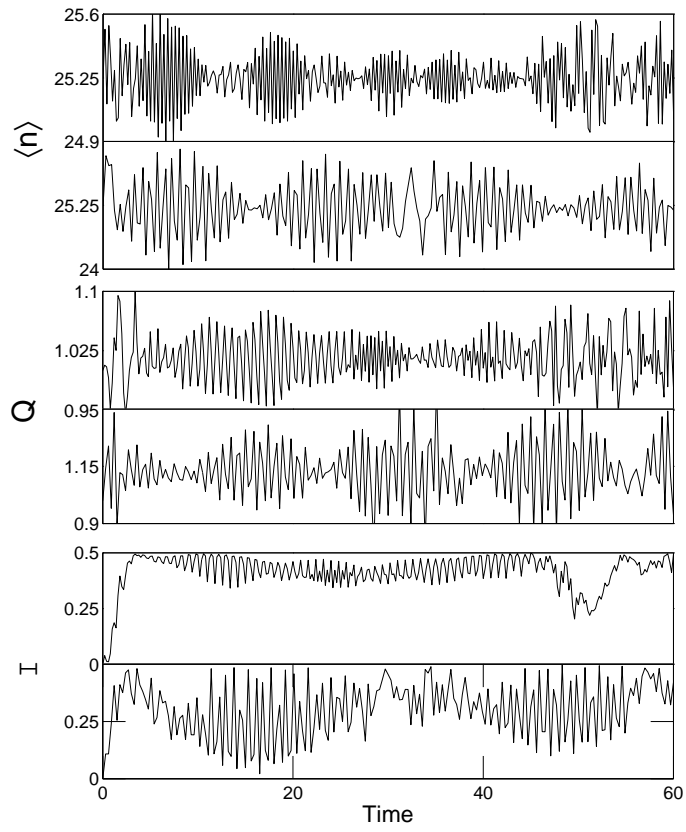


FIG. 2. The same as in Fig. 1 but for $\eta = 0.5$ and $\alpha = (5, 0.5)$.

Now we compare the deeper LDL regime of $\eta = 0.1$. As shown in Figs. 3 and 4, noticeable errors with MRWA were still found, although at significantly reduced levels as compared with Figs. 1 and 2.

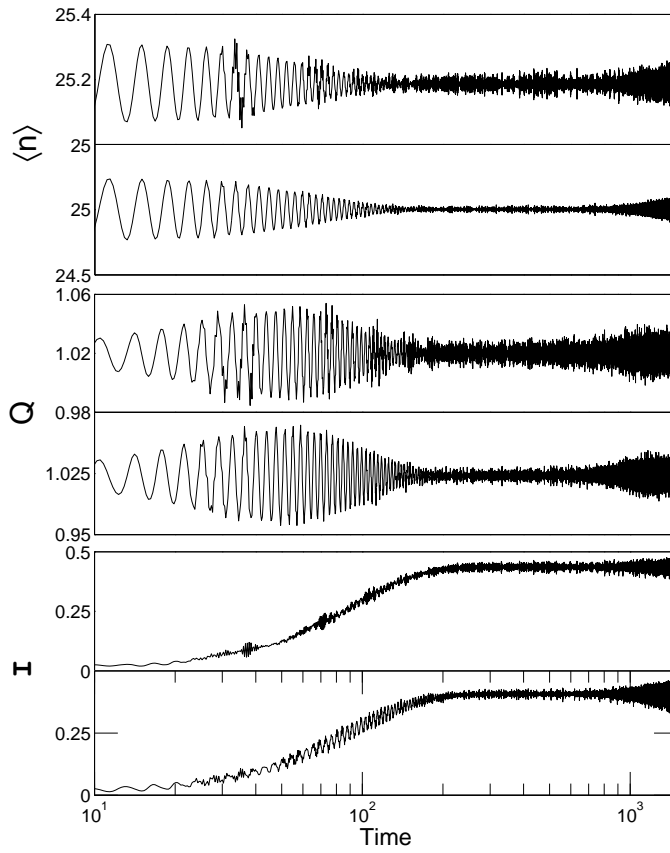


FIG. 3. The same as in Fig. 1 but for $\eta = 0.1$ and $\alpha = (0.5, 5)$. Note the super-revivals for Q .

Figure 4 compares early time dynamics for the same $\eta = 0.1$ but with $\alpha = (5, 0.5)$. We note that the $\mathcal{I} = 0$ value predicts the existence of Schrodinger cat states from both MRWA and NDM results [18]. Also the agreement for $\langle n \rangle$ and Q are better than the case of $\alpha = (0.5, 5)$. These results show clearly that errors in MRWA are sensitive to the phase of the initial coherent state amplitude.

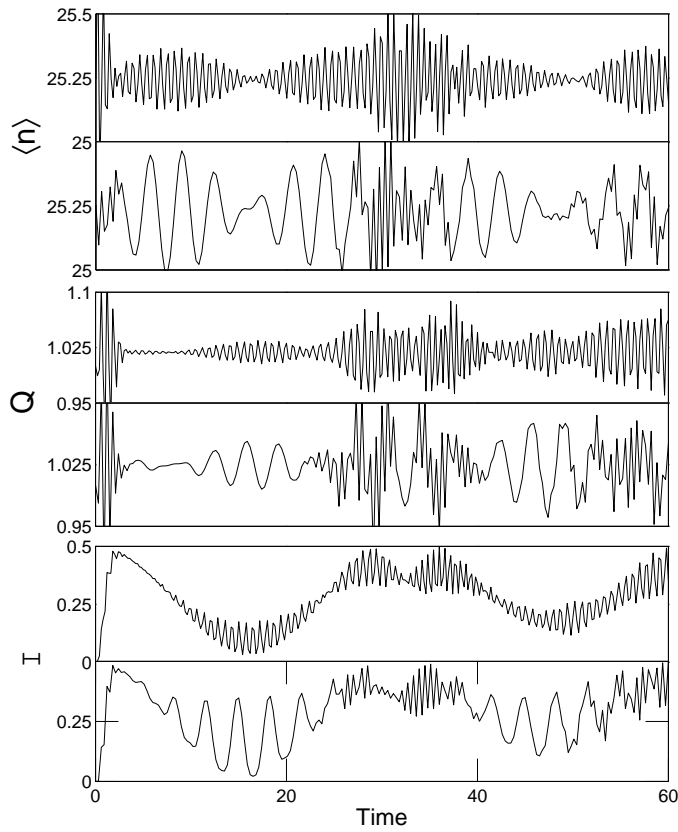


FIG. 4. The same as in Fig. 1 but for $\eta = 0.1$ and $\alpha = (5, 0.5)$.

To further elucidate effects of MRWA, we have carried out additional comparisons. In Fig. 2 and in Fig. 4, we notice that MRWA results predict larger oscillations than the actual smoother behavior of $\langle n \rangle$, Q , and I . This observation is in contrast to our expectations that stem from the effects of RWA in the usual JCM. Let us first recall what is the effect of neglecting counter-rotating terms in the H_{JCM} . For comparison, we consider an initial condition of the form $\tilde{T}\psi(0)$. The results obtained by propagating H_{JCM} dynamically with and without counter-rotating terms are given in Fig. 5. We see H_{JCM} with RWA predicts smoother behavior while the actual H_{JCM} results carry small nutations due to counter-rotating effects. For the ion-trap system displayed in Fig. 6, the results are just the opposite. In ion-trap Hamiltonian MRWA results carry more nutations than the actual smoother behavior. The basic difference between the JCM and the ion-trap system is the requirement of the additional back transformation for the latter via \tilde{T}^\dagger in determining the wave function evolution. From the physical point of view, this transformation brings back the effect of multiple-phonon transitions, present in the ion-trap case, after a simplified single phonon transition dynamics has been determined conveniently in the interaction picture. Neglecting counter-rotating terms in the effective single-phonon model Eq. (13), however, ignores too many multiple-phonon processes at the end of the transformation, thus introduce more noise around the otherwise smoother collapse-revival patterns. We note that this (MRWA in ion-trap models) is opposite to effects of the RWA in the JCM and has been found for an initial motional state with almost real coherent state amplitudes, i.e. $\beta \approx 0$.

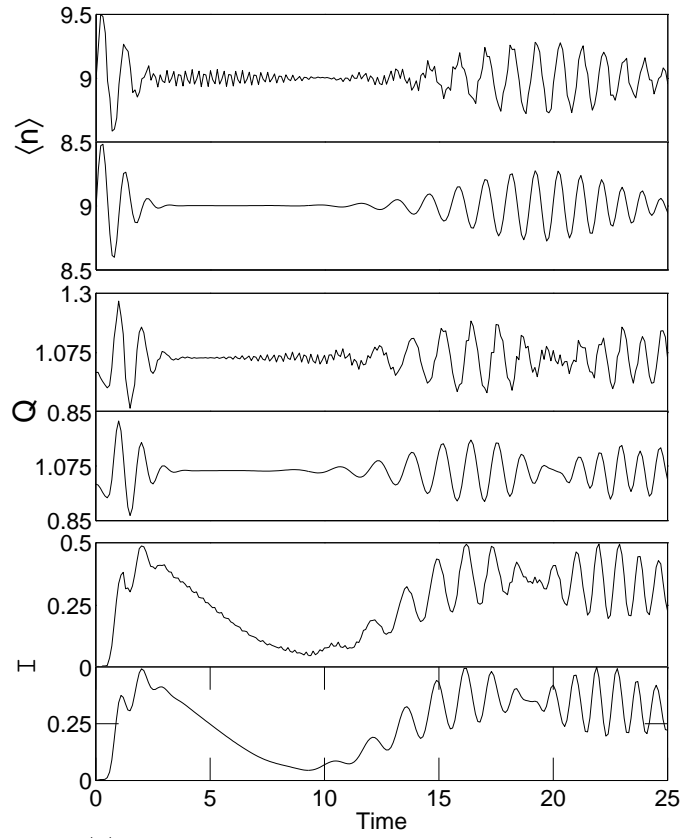


FIG. 5. The mean phonon number $\langle n \rangle$, the Mandel-Q factor, and the impurity parameter \mathcal{I} with $\eta = 0.1$ and $\alpha = (3, 0)$ for the simple single-phonon JCM H_{JCM} with and without RWA. In both cases no back transformation is employed but an initial condition of the form $\tilde{T}\psi(0)$ has been used to compare with the multiple-phonon transition effects in Fig. 6. Within each sub-figure, the upper (lower) part is for H_{JCM} with (without) counter rotating terms.

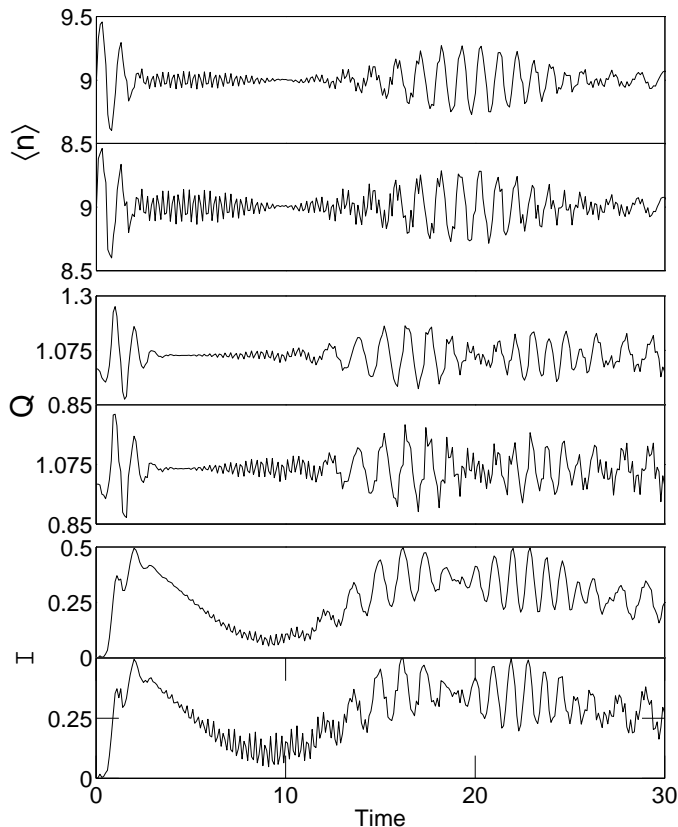


FIG. 6. The same as in Fig. 5 but now for the full ion-trap Hamiltonian which includes multiple phonon transition effects. Within each sub-figure, the upper (lower) curve is obtained by NDM (MRWA).

VI. CONCLUSION

We have investigated the regimes of validity for MRWA of a trapped particle under its coherent interaction with a plane wave laser field. Our study is based on a family of general unitary transformations that incorporate several earlier transforms as special cases [3,7]. This general transformation facilitates the linearization of the system Hamiltonian including the particle's motional degrees of freedom. In model studies presented here, two distinct dynamical regimes appear, the single-phonon dynamics and the double-phonon dynamics. The single phonon model is standard in the deep LDL. The two-phonon model, on the other hand, does not impose any restrictions on the Lamb-Dicke parameter. Thus, addressing validity regimes of MRWA is only necessary for the single-phonon dynamics used extensively in the literature. For this aim, we have employed a numerical diagonalization procedure (without MRWA) and comparatively assessed the validity conditions of MRWA. We find that remarkable errors exist in regimes where MRWA was believed to be applicable. Furthermore, our simulations show that the accuracy and detailed quantitative effects of MRWA depends on the phase of the initial motional coherent state. When this phase is close to zero, time averaged mean phonon number $\langle n \rangle$ displays improved agreement with MRWA results. The agreement however is far from perfect even in the deep LDL. Qualitatively, for almost real initial coherent state amplitude, the counter rotating terms in ion-trap model lead to smoother dynamical behaviors than the results obtained under MRWA, which introduces more larger nutations around the actual more smooth dynamical patterns. This is in stark contrast to CRT effects in usual JCM problems. Physically, this effect arises because of the existence of multiple transitions in motional states. Our study indicates that the connection between cavity QED and ion-trap systems in JCM-type formalisms are possible as long as ranges of the Lamb-Dicke parameter are carefully analyzed to enforce the validity of MRWA.

VII. ACKNOWLEDGMENT

This work is supported by a grant from the National Security Agency (NSA), Advanced Research and Development Activity (ARDA), and the Defense Advanced Research Projects Agency (DARPA) under Army Research Office (ARO)

- [1] M. Fang, S. Swain, and P. Zhou, Phys. Rev. A **63**, 013812 (2001).
- [2] D. Jonathan, M. B. Plenio, and P. L. Knight, Phys. Rev. A **62**, 042307 (2000).
- [3] H. Moya-Cessa, A. Vidiella-Barranco, J. A. Roversi, D. S. Freitas, and S. M. Dutra, Phys. Rev. A **59**, 2518 (1999).
- [4] Y. Wu and X. Yang, Phys. Rev. Lett. **78**, 3086 (1997).
- [5] S. Mancini, H. Moya-Cessa, and P. Tombesi, J. Mod. Opt. **47**, 2133 (2000).
- [6] J. I. Cirac, A. S. Parkins, R. Blatt, and P. Zoller, Adv. At. Mol. Opt. Phys. **37**, 237 (1996).
- [7] L. You, Phys. Rev. A **64**, 012302 (2001).
- [8] E. A. Tur, Optics and Spectroscopy **89**, 574 (2000).
- [9] M. F. Fang and P. Zhou, J. Mod. Opt. **42**, 1199 (1995).
- [10] J. Seke, Nuovo Cimento **16**, 303 (1994).
- [11] R. H. Xie, Q. Rao, D. H. Liu, and G. O. Xu, Nuovo Cimentot D **18**, 405 (1996).
- [12] M. Lewenstein, L. You, J. Cooper, and K. Burnett, Phys. Rev. A **50**, 2207 (1994).
- [13] P. Drummond, Phys. Rev. A **35**, 4253 (1987).
- [14] C. Cohen-Tannoudji, J. Dupont-Roc, and G. Grynberg, *Atom-Photon Interactions*, (John-Wiley and Sons, Inc., New York, 1992).
- [15] J. Ye *et al.*, Phys. Rev. Lett. **83**, 4987 (1999); D. W. Vernooy and H. J. Kimble, Phys. Rev. A **56**, 4287 (1997).
- [16] J.S. Peng and G.X. Li, Phys. Rev. A **47**, 3167 (1993); K. Zaheer and M. S. Zubairy, *ibid.* **37**, 1628 (1988).
- [17] M. O. Scully and M. S. Zubairy, *Quantum Optics*, (Cambridge University Press, New York, 1997).
- [18] J. Gea-Banacloche, Phys. Rev. Lett. **65**, 3385 (1990); Phys. Rev. A **44**, 5913 (1991); S. J. Phoenix and P. L. Knight, *ibid.* **44**, 6023 (1991); P. L. Knight and B. W. Shore, *ibid.* **48**, 642 (1993).
- [19] T. Wong, O. E. Mustecaplioglu, L. You, and M. Lewenstein Phys. Rev. A **61**, 041604 (2000).

